(1961)].
[41]P. Fulde, L. L. Hirst, and A. Luther, Z. Physik 230, 155 (1970).
[42]B. Giovannini, Phys. Letters 26A, 80 (1967).
[43]D. Davidov and D. Shaltiel, Phys. Rev. Letters 21, 1752 (1968).
[44]H. Cottet, P. Donze, J. Dupraz, B. Giovannini, and M. Peter, Z. Angew Phys. 24, 249 (1968).
[45]D. Davidov, R. Orbach, C. Rettori, and E. P. Chock (unpublished).
[46]J. R. Asik, M. A. Ball, and C. P. Slichter, Phys. Rev. 181, 645 (1969); 181, 662 (1969).
[47]M. A. Huisjen, J. F. Siebert, and R. H. Silsbee, *Magnetism and Magnetic Materials* (AIP, New York, 1971), p. 1214.
[48]Y. Yafet, J. Appl. Phys. 39, 853 (1968).
[49]As shown in Table II, the values for σ observed by Asik *et al.* for Li:Au and Na:Au dilute alloys are larger by a factor of 5–10 relative to those observed by us for Al:Au. As was pointed out in the text, metallurgical difficulties might be the reasons for this difference (i.e., the effective Au or Gd concentration due to inhomogeneities in the high-concentration samples may be much less than the nominal. This may be especially true here because the samples were not prepared from a master.) However, it should be stressed that the tendency described in Table II is expected because the difference in valence between the Au impurity and the Al (−2) causes a strong repulsive potential for the conduction electrons. This will reduce the overlap integrals and thus the spin-flip cross section of Al:Au relative to that of Na:Au. (For this alloy the difference in valence is zero.) In a future publication we hope to report more accurate values for σ.
[50]M. H. Cohen and V. Heine, Phys. Rev. 122, 1821 (1961).
[51]C. P. Flynn, D. A. Rigney, and J. A. Gardner, Phil. Mag. 15, 1255 (1967).
[52]B. Caroli, P. Lederer, and D. Saint-James, Phys. Rev. Letters 23, 700 (1969).
[53]L. Dworin and A. Narath, Phys. Rev. Letters 25, 1287 (1970).
[54](a) M. B. Salamon, Phys. Rev. Letters 26, 704 (1971); (b) A. Narath (private communication).
[55]C. Kittel, Solid State Phys. 22, 1 (1968).
[56]R. E. Watson and A. J. Freeman, in *Hyperfine Interactions*, edited by A. J. Freeman and R. B. Frankel (Academic, New York, 1962), p. 53.

PHYSICAL REVIEW B VOLUME 7, NUMBER 1 1 JANUARY 1973

Theoretical Description of the Proton Magnetic Resonance Line Shapes of Ammonium Ions under the Influence of Tunneling*

A. Watton and H. E. Petch
Department of Physics, University of Waterloo, Waterloo, Ontario, Canada
(Received 31 May 1972)

A theoretical treatment for the NMR absorption line shape of a tetrahedral group of protons under the influence of tunneling has been developed for the particular case of NH_4^+ ions. For the applied field parallel to a twofold axis of the ion the derived line shapes depend on a single splitting parameter J. This is a measure of the tunneling splitting of the torsional ground state in comparison to the dipolar energy of the ion. As J varies from 0 to ∞ the calculated line shapes are found to vary between the limiting cases of the distinguishable proton (four spin $\frac{1}{2}$) and indistinguishable proton (spin isomeric) situations, respectively. These theoretical line shapes are compared with the observed "rigid-lattice" line shapes reported for the halides NH_4Cl, NH_4Br, and NH_4I. NH_4Cl and NH_4Br are found to be consistent with $J=0$ although the line shape of the latter exhibits an unexplained departure near the center of the resonance. NH_4I is found to exhibit observable splitting effects ($J=3.3$) in which tunneling has displaced one absorption component sufficiently into the wings to be resolved.

I. INTRODUCTION

The problem of the low-temperature NMR absorption line shape for a four-proton group has been considered by a number of authors. Bersohn and Gutowsky[1] calculated the line shape for a system of four-spin-$\frac{1}{2}$ protons (the so-called four-spin-$\frac{1}{2}$ system) in an ammonium ion (NH_4^+) and used their results to explain the line shapes observed in a single crystal of NH_4Cl at $-195\,^\circ C$. Itoh *et al.*[2] performed an essentially similar calculation, but included the nitrogen-proton interaction to discuss the line shapes of single crystals of NH_4Cl and NH_4Br at $90\,^\circ K$. They found good agreement between the theoretical and experimental line shapes for NH_4Cl, but not so good for NH_4Br.

In order to explain the narrow absorption line observed in solid methane at 1.29 and 1.42 °K, Tomita[3] calculated the line shape for a four-proton system on the basis that the total spin of the molecule ($I=0, 1, 2$) was a good quantum number. These two theories have been compared by Watton *et al.*[4] in the discussion of the line shapes of a group of ammonium salts. They point out that the four-spin-$\frac{1}{2}$ and nuclear-spin-isomeric pictures are just limiting cases of particle distinguishability. The

four-spin-$\frac{1}{2}$ picture is valid when the protons are completely distinguishable over the characteristic time of the experiment (of the order of the inverse linewidth in this case), while the concept of nuclear-spin-isomeric states is valid when the protons are completely indistinguishable over this time.

The simpler problem of tunneling of a three-proton system (methyl group) has been treated by Apaydin and Clough,[5] some of whose ideas are utilized in this paper. However, the four-proton (ammonium ion) case is complicated by the three-dimensional nature of the problem (three Euler angles are needed to specify the orientation of an ammonium ion as opposed to one azimuthal angle for a methyl group). Further complications result from the crystal-field symmetry and the presence of the nitrogen nucleus. These points will be further clarified in the following treatment of the four-proton system.

II. THEORY

The spectra for a system of four interacting protons (spin $\frac{1}{2}$) in a rigid tetrahedral configuration were previously calculated by considering only spin effects on the line shape.[1-4] This paper incorporates the spatial effects of tunneling of the proton group, in this case an ammonium ion, on the spectra.

Since the ion is internally rigid we need only consider the substitution group on the protons which is isomorphic to the tetrahedral group T corresponding to real rotations of the ion. The irreducible representations of this group are labeled A, E^a, E^b, and F, where A, E^a, and E^b are one dimensional and F is three dimensional. The character table for this group is given in Table I and the explicit matrix representation chosen is shown in Table II.

A. Wave Functions

The 16 spin states (ϕ) for the four-proton group in a large applied magnetic field H_0 can be characterized by specifying the components m_i ($=\pm\frac{1}{2}$) of each spin along H_0, i.e., the states can be denoted by $|m_1 m_2 m_3 m_4\rangle$. Also, if $\psi(E)$ represents a normalized torsional ground state of the ion in the crystal field, there are 12 equivalent states $\psi(R)$ obtained from $\psi(E)$ by the 12 operations R (particle permutations) of the group T.

The spin and space states can be reduced with respect to the group T by projecting out of each, those parts which belong to the various rows of the various irreducible representations. In this context, the projection operators for the A, E^a, and E^b states are,[6] apart from a constant factor,

$$P^A = \sum_R R\,, \tag{1a}$$

$$P^{E^a} = \sum_R \chi^{E^a}(R)^* R\,, \tag{1b}$$

$$P^{E^b} = \sum_R \chi^{E^b}(R)^* R\,, \tag{1c}$$

and the projection operator for the ith row of the Fth irreducible representation is[7]

TABLE I. Character table for tetrahedral group T. $\epsilon = e^{2\pi i/3}$.

T	E	$C_2(3)$	$C_3(4)$	$C_3^2(4)$
A	1	1	1	1
E^a	1	1	ϵ	ϵ^2
E^b	1	1	ϵ^2	ϵ
F	3	−1	0	0

TABLE II. Representation of tetrahedral group T.

Rotation[a]	Permutation	χ^A	χ^{E^a}	χ^{E^b}	D_{ij}
E	(1) (2) (3) (4)	1	1	1	1 0 0
					0 1 0
					0 0 −1
$C_2(x)$	(14) (23)	1	1	1	1 0 0
					0 −1 0
					0 0 −1
$C_2(y)$	(13) (24)	1	1	1	−1 0 0
					0 1 0
					0 0 −1
$C_2(z)$	(12) (34)	1	1	1	−1 0 0
					0 −1 0
					0 0 1
$C_3(\bar{x}y\bar{z})$	(134)	1	ϵ^2	ϵ	0 0 1
					1 0 0
					0 1 0
$C_3^2(\bar{x}y\bar{z})$	(143)	1	ϵ	ϵ^2	0 1 0
					0 0 1
					1 0 0
$C_3(xy\bar{z})$	(243)	1	ϵ^2	ϵ	0 0 −1
					1 0 0
					0 −1 0
$C_3^2(xy\bar{z})$	(234)	1	ϵ	ϵ^2	0 1 0
					−1 0 0
$C_3(x\bar{y}z)$	(123)	1	ϵ^2	ϵ	0 0 1
					−1 0 0
					0 −1 0
$C_3^2(x\bar{y}z)$	(132)	1	ϵ	ϵ^2	0 −1 0
					0 0 −1
					1 0 0
$C_3(\bar{x}yz)$	(142)	1	ϵ^2	ϵ	0 0 −1
					−1 0 0
					0 1 0
$C_3^2(\bar{x}yz)$	(124)	1	ϵ	ϵ^2	0 −1 0
					0 0 1
					−1 0 0

[a]The rotation axis is specified in the rotation symbol, e.g., $C_3(xy\bar{z})$ means a threefold rotation around the axis represented by (1, 1, $\bar{1}$) in Fig. 1.

$$P^F_{ni} = \sum_R D_{ni}(R^{-1})R \,, \tag{1d}$$

where $\chi^{E^a}(R)$, $\chi^{E^b}(R)$, $D_{ij}(R)$ are the E^a, E^b, and F representations, respectively, given in Table II.

It should be noted that applying (1d) to an arbitrary function f produces three sets of three functions $f^F_{ni} = P^F_{ni} f$ such that each set with the same n form a basis for the irreducible representation F, i.e.,

$$R f^F_{ni} = \sum_j f^F_{nj} D_{ji}(R) \quad \text{for any } R \in T \,. \tag{2}$$

Using the projection operators of Eqs. (1), the 16 spin states can be reduced to the members $5A + E + 3F$. This reduction of the spin basis is shown in Table III, where the normalized symmetry-adapted basis states are represented by ϕ^{Am}, $\phi^{E^a m}$, $\phi^{E^b m}$, and ϕ^{Fm}_i $(i = 1, 2, 3)$. Here $m = \sum_i m_i$ labels the magnetic substate and takes the values 2, 1, 0, −1, −2. However, since the reduction for $-m$ is of exactly the same form as for $+m$, only the positive m bases are shown.

In a similar manner, the 12 functions $\psi(R)$ can be reduced to the members $A + E + 3F$, where

$$\psi^A = N_A^{-1/2} P^A \psi(E) = N_A^{-1/2} \sum_R \psi(R) \,, \tag{3a}$$

$$\psi^{E^a} = N_E^{-1/2} P^{E^a} \psi(E) = N_E^{-1/2} \sum_R \chi^{E^a}(R)^* \psi(R) \,, \tag{3b}$$

$$\psi^{E^b} = N_E^{-1/2} P^{E^b} \psi(E) = N_E^{-1/2} \sum_R \chi^{E^b}(R)^* \psi(R) \,, \tag{3c}$$

$$\psi^F_{ni} = N_F^{-1/2} P^F_{ni} \psi(E) = N_F^{-1/2} \sum_R D_{ni}(R^{-1}) \psi(R) \,, \tag{3d}$$

where R operating on $\psi(E)$ has been written $\psi(R)$. The N_A, N_E, and N_F are normalizing factors and are given, in a tetrahedral or higher crystal field, by (Appendix A)

$$N_A = 12(1 + 3s_2 + 8s_3) \,,$$

$$N_E = 12(1 + 3s_2 - 4s_3) \,,$$

$$N_F = 4(1 - s_2) \,,$$

where s_2 and s_3 are the overlap integrals for twofold and threefold rotations;

$$s_2 = \langle \psi(E) | \psi(C_2) \rangle, \quad s_3 = \langle \psi(E) | \psi(C_3) \rangle \,.$$

Now protons are fermions and so the total wave function Ψ consisting of both spin and spatial variables must be antisymmetric under any interchange of two protons or, equivalently, symmetric under any tetrahedral reorientation since this corresponds to an interchange of two pairs of protons. Hence when we form the product representation of space and spin ($\psi \times \phi$—assuming vibrational and electronic parts are in their symmetric ground state), we must project out of $\psi \times \phi$ only that part which transforms according to the irreducible representation A of T. From the character table (Table I) it can be seen that only the combinations $A \times A$, $E^a \times E^b$, $E^b \times E^a$, and $F \times F$ contain such a symmetric part. Hence the appropriately normalized ground states satisfying the criteria for wavefunction symmetry are

$$\Psi^{Am} = \psi^A \phi^{Am} \,, \tag{4a}$$

$$\Psi^{E^a m} = \psi^{E^a} \phi^{E^b m} \,, \tag{4b}$$

$$\Psi^{E^b m} = \psi^{E^b} \phi^{E^a m} \,, \tag{4c}$$

$$\Psi^{Fm}_n = 3^{-1/2} \sum_k \psi^F_{nk} \phi^{Fm}_k \,. \tag{4d}$$

The last expression (4d) can be seen by considering the projection operator P^A acting on any term $\psi^F_{ni} \phi^{Fm}_j$ of the unreduced product $\psi \times \phi$:

$$P^A \psi^F_{ni} \phi^{Fm}_j = \sum_R R(\psi^F_{ni} \phi^{Fm}_j)$$

TABLE III. Reduction of spin basis to symmetry-adapted form. α_i, β_i denote spin up and spin down, respectively, for proton i.

$$\begin{pmatrix} \phi^{A2} \\ 2\,\phi^{A1} \\ 2\,\phi^{F1} \\ 2\,\phi^{F1}_2 \\ 2\,\phi^{F1}_3 \\ \sqrt{6}\,\phi^{A0} \\ \sqrt{6}\,\phi^{E^a 0} \\ \sqrt{6}\,\phi^{E^b 0} \\ \sqrt{2}\,\phi^{F0}_1 \\ \sqrt{2}\,\phi^{F0}_2 \\ \sqrt{2}\,\phi^{F0}_3 \end{pmatrix} = \begin{pmatrix} 1 & & & & & & & & & & & \\ & 1 & 1 & 1 & 1 & & & & & & & \\ & 1 & -1 & -1 & 1 & & & & & & & \\ & 1 & -1 & 1 & -1 & & & & & & & \\ & -1 & -1 & 1 & 1 & & & & & & & \\ & & & & & 1 & 1 & 1 & 1 & 1 & 1 & \\ & & & & & 1 & \epsilon^2 & \epsilon & \epsilon & \epsilon^2 & 1 & \\ & & & & & 1 & \epsilon & \epsilon^2 & \epsilon^2 & \epsilon & 1 & \\ & & & & & 0 & 0 & 1 & -1 & 0 & 0 & \\ & & & & & 0 & 1 & 0 & 0 & -1 & 0 & \\ & & & & & -1 & 0 & 0 & 0 & 0 & 1 & \end{pmatrix} \begin{pmatrix} \alpha_1\alpha_2\alpha_3\alpha_4 \\ \beta_1\alpha_2\alpha_3\alpha_4 \\ \alpha_1\beta_2\alpha_3\alpha_4 \\ \alpha_1\alpha_2\beta_3\alpha_4 \\ \alpha_1\alpha_2\alpha_3\beta_4 \\ \beta_1\beta_2\alpha_3\alpha_4 \\ \beta_1\alpha_2\beta_3\alpha_4 \\ \beta_1\alpha_2\alpha_3\beta_4 \\ \alpha_1\beta_2\beta_3\alpha_4 \\ \alpha_1\beta_2\alpha_3\beta_4 \\ \alpha_1\alpha_2\beta_3\beta_4 \end{pmatrix}$$

$$= \sum_{kl} \psi^F_{nk} \phi^{Fm}_l \sum_R D_{kl}(R) D_{lj}(R)$$

by Eq. (2);

$$P^A \psi^F_{ni} \phi^{Fm}_j = 4 \sum_{kl} \psi^F_{nk} \phi^{Fm}_l \delta_{kl} \delta_{ij}$$

by the orthogonality theorem of group theory[6];

$$P^A \psi^F_{ni} \phi^{Fm}_j = 4 \sum_k \psi^F_{nk} \phi^{Fm}_k \delta_{ij} \ .$$

Hence, Eq. (4d) results upon normalization.

Having obtained our unperturbed symmetric ground-state wave functions we turn to the consideration of the Hamiltonian for the system.

B. Hamiltonian

The Hamiltonian for the ion situated in a crystal field and large applied magnetic field H_0 can be written

$$\mathcal{H} = \mathcal{H}_R + \mathcal{H}_Z + \mathcal{H}_N + \mathcal{H}'_{pp} + \mathcal{H}'_{pN} \ ,$$

where each term has the following meaning: $\mathcal{H}_R$ is the rotational Hamiltonian consisting of kinetic and potential energy contributions. It is a function of spatial operators only. $\mathcal{H}_Z = -\gamma_p \hbar H_0 \sum_i I^i_z$ is the Zeeman energy of the proton system (I^i_z is the spin component of proton i along H_0). $\mathcal{H}_N = -\gamma_N \hbar H_0 I^N_z$ is the Zeeman energy of the nitrogen nucleus (I^N_z is the spin component of the nitrogen nucleus along H_0).

$$\mathcal{H}'_{pp} = \sum_{i<j} B_{ij} S_{ij} \tag{5a}$$

is the secular part of the proton-proton dipolar interaction;

$$\mathcal{H}'_{pN} = \sum_i B_{i0} S_{i0} \tag{5b}$$

is the secular part of the proton-nitrogen dipolar interaction.

Also

$$B_{ij} = \Gamma_p (1 - 3\cos^2\theta_{ij}) \ , \tag{6a}$$

$$S_{ij} = I^i_z I^j_z - \tfrac{1}{4}(I^i_+ I^j_- + I^i_- I^j_+) \ , \tag{6b}$$

$$B_{i0} = \Gamma_N (1 - 3\cos^2\theta_{i0}) \ , \tag{7a}$$

$$S_{i0} = I^i_z I^N_z \ , \tag{7b}$$

$$\Gamma_p = \frac{\gamma_p^2 \hbar^2}{r_p^3} \ , \quad \Gamma_N = \frac{\gamma_N \gamma_p \hbar^2}{r_N^3} \ ,$$

where θ_{ij} is the angle the proton-proton vector $(\vec{r}_p)_{ij}$ makes with $\vec{H}_0$ and θ_{i0} is the angle the proton-nitrogen vector $(\vec{r}_N)_i$ makes with $\vec{H}_0$. γ_p, γ_N are the proton and nitrogen gyromagnetic ratios, respectively. Note that (6a) and (7a) consist of spatial variables only, while (6b) and (7b) consist of spin variables only.

Now $\mathcal{H}_R$ is completely symmetric with respect to spatial permutations of T and therefore belongs to the irreducible representation A of T. Hence $\mathcal{H}_R$ is diagonal in the representation chosen. The diagonal matrix elements are (Appendix B), for a tetrahedral crystal field,

$$H^A = \langle \Psi^{Am} | \mathcal{H}_R | \Psi^{Am} \rangle = \frac{H_t + 3\Delta_2 + 8\Delta_3}{1 + 3s_2 + 8s_3} \ , \tag{8a}$$

$$H^E = \langle \Psi^{E^a m} | \mathcal{H}_R | \Psi^{E^a m} \rangle = \langle \Psi^{E^b m} | \mathcal{H}_R | \Psi^{E^b m} \rangle$$

$$= \frac{H_t + 3\Delta_2 - 4\Delta_3}{1 + 3s_2 - 4s_3} \ , \tag{8b}$$

$$H^F = \langle \Psi^{Fm}_n | \mathcal{H}_R | \Psi^{Fm}_n \rangle = \frac{H_t - \Delta_2}{1 - s_2} \ , \tag{8c}$$

where

$$H_t = \langle \Psi(E) | \mathcal{H}_R | \psi(E) \rangle \ ,$$

$$\Delta_i = \langle \Psi(E) | \mathcal{H}_R | \psi(C_i) \rangle, \quad i = 2, 3 \ .$$

To facilitate the evaluation of matrix elements of $\mathcal{H}'_{pp}$ and $\mathcal{H}'_{pN}$ it is useful to write these in a symmetry adapted form. There are six terms B_{ij} which can be reduced to the members $A + E + F$, e.g., by applying the projection operators of Eqs. (1) to the element B_{12}, we find

$$B^A = B_{12} + B_{34} + B_{24} + B_{13} + B_{14} + B_{23} \ , \tag{9a}$$

$$B^{E^a} = B_{12} + B_{34} + \epsilon^2 (B_{24} + B_{13}) + \epsilon (B_{14} + B_{23}) \ , \tag{9b}$$

$$B^{E^b} = (B^{E^a})^* \ , \tag{9c}$$

$$B^F_1 = B_{14} - B_{23} \ , \tag{9d}$$

$$B^F_2 = B_{13} - B_{24} \ , \tag{9e}$$

$$B^F_3 = B_{34} - B_{12} \ , \tag{9f}$$

where $\epsilon = e^{2\pi i/3}$. The labeling convention here and for all symmetry adapted forms used in this paper is exactly analogous to that employed for ψ and ϕ states previously [cf. Eqs. (4) and Table III]. Exactly equivalent expressions can be obtained for the symmetry adapted spin parts S^A, etc., by applying the projection operators of Eqs. (1) to the spin element S_{12}.

Similarly, the four elements B_{i0} in the nitrogen contribution can be reduced to the members $A + F$ by applying the projection operators to B_{10} to give

$$B^A_N = B_{10} + B_{20} + B_{30} + B_{40} \ , \tag{10a}$$

$$B^F_{N1} = B_{10} - B_{20} - B_{30} + B_{40} \ , \tag{10b}$$

$$B^F_{N2} = B_{10} - B_{20} + B_{30} - B_{40} \ , \tag{10c}$$

$$B^F_{N3} = -B_{10} - B_{20} + B_{30} + B_{40} \ , \tag{10d}$$

with equivalent expressions for the symmetry adapted spin parts S^A_N, etc. The subscript N distinguishes these as the nitrogen contribution.

Now $\mathcal{H}'_{pp}$ and $\mathcal{H}'_{pN}$ are completely symmetric under simultaneous spin and space permutations (particle permutations) and, therefore, belong to the A representation of T in the product space. Therefore, from the character table (Table I), the space (B) and spin (S) parts of the dipolar interactions occur only in the combinations $B^A S^A$,

$B^{E^a}S^{E^b}$, $B^{E^b}S^{E^a}$, and $B^F S^F$. Using the projection operators [Eq. (1)] to project the A part out of the $B\times S$ product representation in the same way that led to Eqs. (4), it can be shown that $\mathcal{H}'_{pp}$ and $\mathcal{H}'_{pN}$ [Eqs. (5)] can be written

$$\mathcal{H}'_{pp}=\tfrac{1}{6}B^A S^A+\tfrac{1}{6}B^{E^a}S^{E^b}+\tfrac{1}{6}B^{E^b}S^{E^a}+\tfrac{1}{2}\sum_k B_k^F S_k^F\,, \tag{11a}$$

$$\mathcal{H}'_{pN}=\tfrac{1}{4}B_N^A S_N^A+\tfrac{1}{4}\sum_k B_{Nk}^F S_{Nk}^F\,. \tag{11b}$$

C. Matrix Elements of $\mathcal{H}'_{pp}$

Having reduced both our wave functions and Hamiltonian into symmetry adapted forms, standard theorems in group theory[6] can be employed to simplify the evaluation of matrix elements. For example, consider the matrix element of $\mathcal{H}'_{pp}$ between F states since this is the most complicated. The techniques employed, however, apply to all matrix elements. Note that since $\mathcal{H}'_{pp}$ commutes with $\mathcal{H}_Z$ (is secular), it is necessarily diagonal with respect to the quantum number m.

Since from the character table (Table I) $A\times F=F$, $E^a\times F=F$, $E^b\times F=F$, and $F\times F=A+E+2F$ and all matrix elements transform like A (are invariant under permutations because they are just numbers), then all parts of $\mathcal{H}'_{pp}$ in Eq. (11a) contribute to $\langle\Psi_n^{Fm}|\mathcal{H}'_{pp}|\Psi_{n'}^{Fm}\rangle$.

Consider the first term

$$\tfrac{1}{6}\langle\Psi_n^{Fm}|B^A S^A|\Psi_{n'}^{Fm}\rangle = \tfrac{1}{18}\sum_{ij}\langle\psi_{ni}^F|B^A|\psi_{nj}^F\rangle\langle\phi_i^{Fm}|S^A|\phi_j^{Fm}\rangle \tag{12}$$

from Eq. (4d). Similar expressions for the other terms and other matrix elements can be obtained and in principle be evaluated. However, let us at this point make the simplifying assumption that the overlaps (s_2 or s_3) $\langle\psi(E)|\psi(R)\rangle\ll 1$ for $R\neq E$, i.e., the ion is fairly well localized in the crystal field. This condition means that matrix elements of $\mathcal{H}'_{pp}$ between states of different orientation can be neglected in comparison to matrix elements between states of the same orientation. This is not to say that $\langle\psi(E)|\mathcal{H}_R|\psi(R)\rangle$ for $R\neq E$ (i.e., Δ_2 or Δ_3) can be neglected as small since $\mathcal{H}_R\gg\mathcal{H}'_{pp}$. Substituting in Eq. (12) from Eq. (3d) and making the above approximation gives

$$\tfrac{1}{6}\langle\Psi_n^{Fm}|B^A S^A|\Psi_{n'}^{Fm}\rangle=\tfrac{1}{6}B^A S_{F\alpha F\alpha}^{Am}\delta_{nn'}\,,$$

where $S_{F\alpha F\alpha}^{Am}=\langle\phi_{F\alpha}^m|S^A|\phi_{F\alpha}^m\rangle$ has been introduced for convenience in writing ($\alpha=1$, 2, or 3).

Similarly, the other terms of this matrix element are

$$\tfrac{1}{6}\langle\Psi_n^{Fm}|B^{E^a}S^{E^b}|\Psi_{n'}^{Fm}\rangle = \tfrac{1}{18}B^{E^a}(S_{F1F1}^{E^bm}+\epsilon S_{F2F2}^{E^bm}+\epsilon^2 S_{F3F3}^{E^bm})\times(\delta_{n1}+\epsilon^2\delta_{n2}+\epsilon\delta_{n3})\delta_{nn'}$$

$$=\tfrac{1}{6}\langle\Psi_n^{Fm}|B^{E^b}S^{E^a}|\Psi_{n'}^{Fm}\rangle^*\,,$$

where

$$S_{F\alpha F\alpha}^{E^bm}=\langle\phi_{F\alpha}^m|S^{E^b}|\phi_{F\alpha}^m\rangle\,;$$

$$\tfrac{1}{2}\sum_k\langle\Psi_n^{Fm}|B_k^F S_k^F|\Psi_n^{Fm}\rangle=0\,;$$

and

$$\tfrac{1}{2}\sum_k\langle\Psi_n^{Fm}|B_k^F S_k^F|\Psi_{n'}^{Fm}\rangle=\tfrac{1}{6}B_{n'}^F(S_{F2F3}^{F1m}+S_{F3F1}^{F2m}+S_{F1F2}^{F3m})\,,$$

where

$$S_{F\alpha F\beta}^{F\gamma m}=\langle\phi_{F\alpha}^m|S_\gamma^F|\phi_{F\beta}^m\rangle$$

and (n,n',n'') are (1, 2, 3) and cyclic permutations.

The spin matrix elements, S^A, etc., are evaluated between the states given in Table III by substitution from Eq. (6b) and the spin equivalent of Eqs. (9) in a straightforward manner. When this is done we end up with the matrix representation of $\mathcal{H}'_{pp}$ shown in Table IV, where

$$a=\tfrac{1}{8}B^A\,, \tag{13a}$$

$$e=\tfrac{1}{4}B^{E^b}\,, \tag{13b}$$

$$b'=-\tfrac{3}{8}B_1^F\,,\quad b=\tfrac{1}{8}B_1^F\,, \tag{13c}$$

$$c'=-\tfrac{3}{8}B_2^F\,,\quad c=\tfrac{1}{8}B_2^F\,, \tag{13d}$$

$$d'=-\tfrac{3}{8}B_3^F\,,\quad d=\tfrac{1}{8}B_3^F\,, \tag{13e}$$

$$f=\tfrac{1}{8}(B_{12}+B_{34}+B_{24}+B_{13}-B_{14}-B_{23})\,, \tag{13f}$$

$$g=\tfrac{1}{8}(B_{12}+B_{34}-B_{24}-B_{13}+B_{14}+B_{23})\,, \tag{13g}$$

$$h=\tfrac{1}{8}(-B_{12}-B_{34}+B_{24}+B_{13}+B_{14}+B_{23})\,. \tag{13h}$$

It can easily be shown that for a tetrahedral configuration, B^A (and hence a)$\equiv 0$ for all orientations.

The matrix in Table IV is equivalent to those developed by previous authors[1-3] with different spin bases.

D. Matrix for $\mathcal{H}'_{pN}$

There are three cases of equal statistical weight depending on whether $m_N=0$, -1, $+1$. For $m_N=0$, $\mathcal{H}'_{pN}=0$ and the nitrogen nucleus makes no contribution to the dipolar interaction. For $m_N=+1$ we

TABLE IV. Matrix representation of $\mathcal{H}'_{pp}$. The elements are defined in the text.

Ψ^{A2}	Ψ^{A1}	Ψ_1^{F1}	Ψ_2^{F1}	Ψ_3^{F1}	Ψ^{A0}	Ψ^{E^a0}	Ψ^{E^b0}	Ψ_1^{F0}	Ψ_2^{F0}	Ψ_3^{F0}
$2a$										
	$-a$	b'	c'	d'						
	b'	f	d	c						
	c'	d	g	b						
	d'	c	b	h						
					$-2a$	e	e^*			
					e^*	0	0			
					e	0	0			
								$-2f$	$-2d$	$-2c$
								$-2d$	$-2g$	$-2b$
								$-2c$	$-2b$	$-2h$

TABLE V. Matrix representation of $\mathcal{H}'_{pN}$. The elements are defined in the text. Blank spaces are zeros.

Ψ^{A2}	Ψ^{A1}	Ψ_1^{F1}	Ψ_2^{F1}	Ψ_3^{F1}	Ψ^{A0}	Ψ^{Eq_0}	Ψ^{Eb_0}	Ψ_1^{F0}	Ψ_2^{F0}	Ψ_3^{F0}
$2a_N$										
	a_N	b'_N	c'_N	d'_N						
	b'_N	f_N	d_N	c_N						
	c'_N	d_N	f_N	b_N						
	d'_N	c_N	b_N	f_N						
					0	0	0	b''_N	c''_N	d''_N
					0	0	0	0	0	0
					0	0	0	0	0	0
					b''_N	0	0	0	0	0
					c''_N	0	0	0	0	0
					d''_N	0	0	0	0	0

can perform an identical treatment to that above for $\mathcal{H}'_{pp}$ and produce the matrix representation for $\mathcal{H}'_{pN}$ given in Table V, where

$$a_N = \tfrac{3}{4} B_N^A , \tag{14a}$$

$$b_N = \tfrac{1}{4} B_{N1}^F , \quad b'_N = -\tfrac{1}{4} B_{N1}^F , \quad b''_N = -\tfrac{1}{6}\sqrt{3}\, B_{N1}^F ; \tag{14b}$$

$$c_N = \tfrac{1}{4} B_{N2}^F , \quad c'_N = -\tfrac{1}{4} B_{N2}^F , \quad c''_N = -\tfrac{1}{6}\sqrt{3}\, B_{N2}^F ; \tag{14c}$$

$$d_N = \tfrac{1}{4} B_{N3}^F , \quad d'_N = -\tfrac{1}{4} B_{N3}^F , \quad d''_N = -\tfrac{1}{6}\sqrt{3}\, B_{N3}^F ; \tag{14d}$$

$$f_N = \tfrac{1}{4} B_N^A , \tag{14e}$$

where again, for a tetrahedral configuration, B_N^A (and hence a_N and f_N) $\equiv 0$ for all orientations.

The matrix for $m_N = -1$ is just the negative of this. Also note that since the matrix for $-m$ is identical to that for $+m$ only the positive m elements are presented in Tables IV and V.

E. Transition Probabilities

The transition probabilities between unperturbed levels induced by an rf magnetic field applied at the Larmor frequency are proportional to the square of the matrix element of I_x ($=\sum_i I_x^i$) between the unperturbed states. These have been shown previously[3,4] to be

$$W^A(\pm 2 \rightleftarrows \pm 1) = |\langle \phi^{A\pm 2} | I_x | \phi^{A\pm 1} \rangle|^2 = 1 , \tag{15a}$$

$$W^A(\pm 1 \rightleftarrows 0) = |\langle \phi^{A\pm 1} | I_x | \phi^{A0} \rangle|^2 = \tfrac{3}{2} , \tag{15b}$$

$$W_i^F(\pm 1 \rightleftarrows 0) = |\langle \phi_i^{F\pm 1} | I_x | \phi_i^{F0} \rangle|^2 = \tfrac{1}{2} . \tag{15c}$$

In the matrices of Tables IV and V and of Eqs. (8) together with the transition probabilities of Eqs. (15) we have all the necessary machinery to calculate the absorption spectra for any crystal orientation. However, the largest matrix to be handled is a 4×4 and cannot be diagonalized analytically. Hence a powder average cannot be obtained in general for arbitrary Δ_2, Δ_3. We shall confine ourselves to the consideration of certain symmetry directions.

An initial simplification will be achieved if it is noted that the diagonal matrix for $\mathcal{H}_R$ of Eqs. (8) can be reduced by any multiple of the unit matrix. Since this shifts all levels by an equal amount the transitions observed between levels will be unaffected. Hence let us reduce each element of Eqs. (8) by H^F so that the new elements become

$$\begin{aligned} J^A &= H^A - H^F = 4(\Delta_2 + 2\Delta_3) , \\ J^E &= H^E - H^F = 4(\Delta_2 - \Delta_3) , \\ J^F &= H^F - H^F = 0 . \end{aligned} \tag{16}$$

F. H_0 Perpendicular to Tetrahedral Edge

Consider H_0 in the z direction of the coordinate system defined by Fig. 1. In this case,

$$\theta_{10} = \theta_{20} = -\theta_{30} = -\theta_{40} = \cos^{-1}(\tfrac{1}{3}\sqrt{3})$$

and hence,

$$B_{10} = B_{20} = B_{30} = B_{40} = 0 .$$

Therefore, for this particular orientation all matrix elements of $\mathcal{H}'_{pN}$ given by Eqs. (10) and (14) are zero. The nitrogen contribution is zero for H_0 along z and equivalent x and y directions.

The B_{ij} terms for this orientation are

$$B_{12} = B_{34} = \Gamma_p ,$$

$$B_{13} = B_{14} = B_{23} = B_{24} = -\tfrac{1}{2}\Gamma_p ,$$

so that the matrix elements for $\mathcal{H}'_{pp}$ [Eqs. (13)] are

$$a = b = b' = c = c' = d = d' = 0 ,$$

$$e = \tfrac{3}{4}\Gamma_p , \quad f = g = \tfrac{1}{4}\Gamma_p , \quad h = -\tfrac{1}{2}\Gamma_p .$$

Thus the $m = 2$ and 1 magnetic submatrices are diagonal while the A and E states are mixed in the $m = 0$ sublevel.

It is a straighforward matter to diagonalize this matrix and obtain transitions at frequencies ν relative to the central transition of

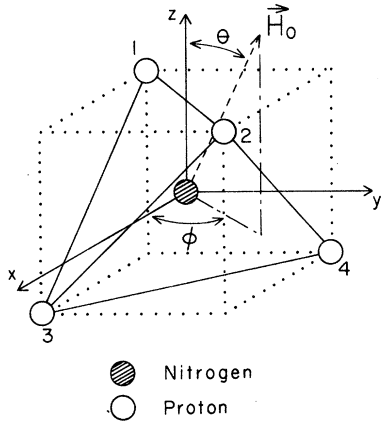

FIG. 1. Coordinate system of NH_4^+ ion. Direction of $\vec{H}_0$ is defined by the polar angles (θ, ϕ).

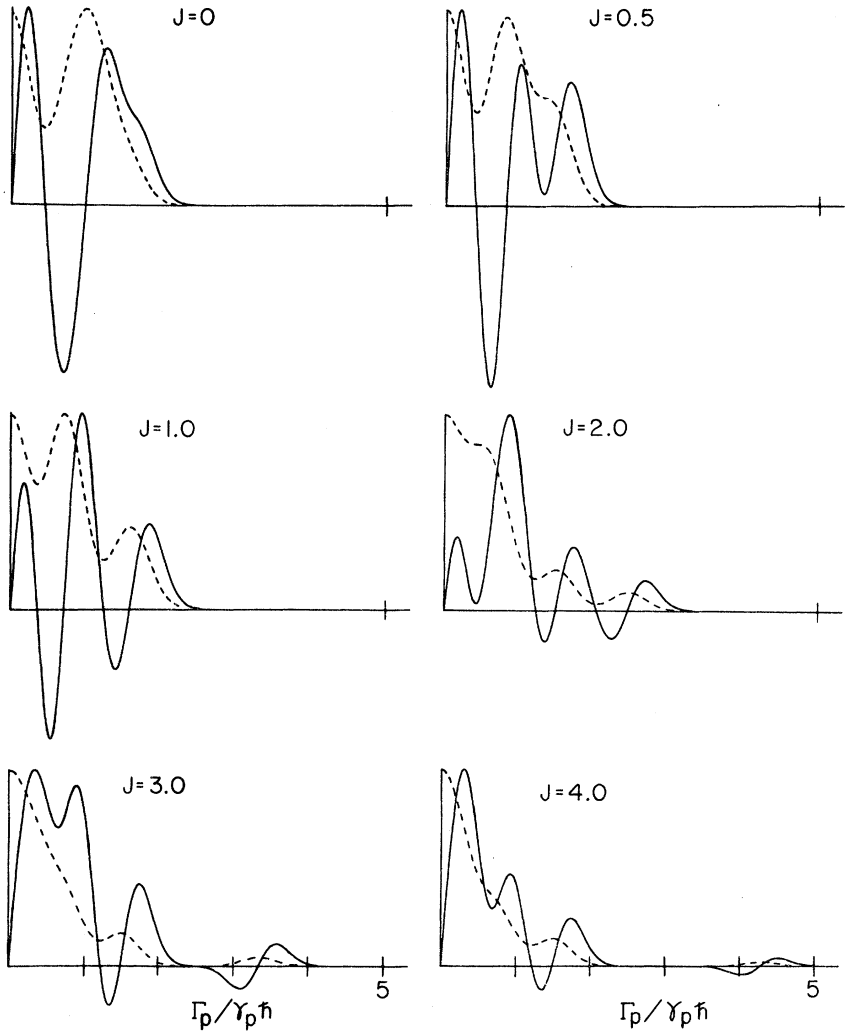

FIG. 2. Absorption (dashed curve) and derivative (solid curve) line shapes calculated for various splitting parameters (J). The magnetic field along the horizontal axis is in units of $\Gamma_p/\gamma_p\hbar$. The broadening factor $\gamma_p^2\hbar^2\langle\Delta H^2\rangle/\Gamma_p^2 = \frac{1}{18}$ and the modulation chosen is $\Gamma_p/12\gamma_p\hbar$. For r_p of 1.68 Å these correspond to $\Gamma_p/\gamma_p\hbar = 6$ G, $\langle\Delta H^2\rangle = 2$ G^2 and a modulation of 0.5 G. (The vertical scale is arbitrary.)

$$h\nu = 0 \text{ with relative intensity } 2\,, \tag{17a}$$

$$h\nu = \tfrac{3}{4}\Gamma_p \text{ with relative intensity } 1\,, \tag{17b}$$

$$h\nu = \pm\tfrac{3}{2}\Gamma_p \text{ with relative intensity } \tfrac{1}{2}\,, \tag{17c}$$

and

$$h\nu = \pm\frac{J}{2}\left[1 \mp \left(1+\frac{9}{2J^2}\right)^{1/2}\right]\Gamma_p$$

with relative intensity

$$\frac{3}{2} - \frac{27}{8J^2}\left[1+\frac{9}{2J^2} \pm \left(1+\frac{9}{2J^2}\right)^{1/2}\right]^{-1}, \tag{17d}$$

where

$$J = \left(\frac{J^A - J^E}{\Gamma_p}\right) = \frac{12\Delta_3}{\Gamma_p} \tag{18}$$

is the splitting parameter.

So far, the effects of surrounding ions have been neglected. These can be included in an approximate way as a Gaussian broadening of the skeletal lines obtained above. This is achieved by convolution of the above lines with a Gaussian function of the form $\langle\Delta H^2\rangle^{-1/2}\exp[-\frac{1}{2}(H-H_c)^2/2\langle\Delta H^2\rangle]$, where H is the magnetic field relative to H_0 and H_c is the magnetic field relative to H_0, at which the transitions defined by Eqs. (17) occur. $\langle\Delta H^2\rangle$ is the interionic contribution to the proton second moment.

The variation of absorption and derivative line shape with splitting parameter J is shown for a number of J values in Fig. 2, where the dimensionless broadening factor $\gamma_p^2\hbar^2\langle\Delta H^2\rangle/\Gamma_p^2 = \frac{1}{18}$ has been chosen. For a proton-proton distance r_p of 1.68 Å (a typical value for ammonium salts) this corresponds to $\langle\Delta H^2\rangle = 2$ G^2, while $\Gamma_p/\gamma_p\hbar = 6$ G.

It should be noted that for the x, y, or z directions considered, not only does the nitrogen contribution vanish, but the final line shape depends only on one splitting parameter J [Eqs. (17) and

(18)]. This is not true for any other direction since, in general, the line shape will depend on both J^A and J^E separately and not just on their difference. For this reason no general dependence of line shape on splitting has been shown for other directions although these are easily obtained for any desired splitting J^A and J^E from the matrices of Eqs. (8) and Tables IV and V.

In a very large crystal field the overlap of the torsional wave function from one "well" to another is very small and $\Delta_3 \ll \Gamma_p$ so that J is essentially zero. In this situation the line shape (Fig. 2) corresponds to that for the four-spin-$\frac{1}{2}$ system discussed by Bersohn and Gutowsky[1] and Itoh *et al.*[2] If the crystal field is reduced the overlap of wave functions increases and J increases. One of the components of Eq. (17d) begins to move out into the wings while the other moves in toward the origin ($H=0$). Eventually, Δ_3 becomes greater than Γ_p and the one component completely disappears into the wings while the other is pushed into the origin. This situation corresponds to the spin-isomeric system discussed by Tomita[3] and Watton *et al.*[4] in which the spin-symmetry types are unmixed (total spin of the ion is a good quantum number). Of course, if the crystal field becomes too low, and the overlap too large then the approximation employed in the neglect of matrix elements like $\langle\psi(E)|\mathcal{H}'_{pp}|\psi(R)\rangle$ for $R \neq E$ breaks down and the line shape will be further modified beyond that for the spin-isomeric type.

G. Tetragonal Crystal Field

The effect of a tetragonal crystal field [see Appendix B, Eq. (B1)] is just to change the diagonal element $\langle\Psi_3^{Fm}|\mathcal{H}_R|\Psi_3^{Fm}\rangle$ from zero to J_3^F. The F submatrix of $\mathcal{H}_R+\mathcal{H}'_{pp}$ for the z direction is diagonal so the $|\Psi_3^{Fm}\rangle$ levels are just shifted by this amount J_3^F from $m=0$ and ± 1. Since there are no transitions from these levels to other levels the observed spectrum for the z direction is unaltered in a tetragonal crystal field.

III. DISCUSSION

It is instructive now to compare the theoretical line shapes obtained with various splitting parameters with those observed in some selected ammonium salts to see if the latter are understandable in terms of the tunneling theory developed here.

The theoretical line shape for zero splitting ($J=0$) is identical to the four-spin-$\frac{1}{2}$ situation discussed by Bersohn and Gutowsky[1] which serves as an adequate description of the low-temperature line shape observed by them in NH_4Cl. In a later study of both NH_4Cl and NH_4Br, Itoh *et al.*[2] found that the four-spin-$\frac{1}{2}$ treatment, while adequate for the line shape of NH_4Cl, was not so good for the line shape of NH_4Br near the center of the resonance. These two materials are structurally very similar.[6,9] Below the λ point (243 °K), NH_4Cl has the CsCl-type structure; all NH_4^+ ions having the same orientation with each nitrogen-proton bond directed towards a nearest-neighbor halogen atom. Below its λ temperature (235 °K), NH_4Br is tetragonal but only slightly distorted from CsCl type. However, below about 78 °K it undergoes a first-order phase transition to the same cubic structure as NH_4Cl.

We have measured the derivative of the proton absorption line shape at 4.2 °K of a single crystal of NH_4Br by the standard cw technique described earlier[4] and have observed a line shape very similar to that reported by Itoh *et al.*[2] In Fig. 3 we compare our experimental line shape for $\vec{H}_0$ in the [100] crystal direction (i.e., along the ionic x axis) to the theoretical line shapes obtained for $J=0$ and 0.7. The line shape for NH_4Cl has not been reproduced in Fig. 3 since the excellent agreement between this and the $J=0$ case has already been established.[1,2] Some comments should be made here on the choice of the broadening factor $\langle\Delta H^2\rangle$. As pointed out by Itoh *et al.*[2] the interionic second moment calculated from the Van Vleck formula is only valid if the interionic dipolar interaction is sufficiently large to broaden the component lines so that they completely overlap. If the interionic interaction is very much smaller than the intraionic interaction the component lines of the spectrum remain resolved with no overlap. In the latter case, those parts of the interionic dipolar interaction which couple states belonging to different

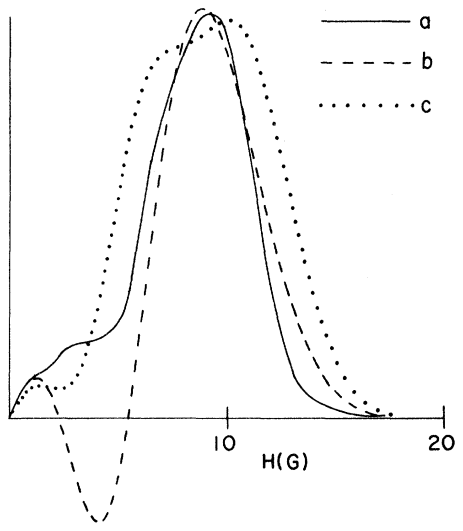

FIG. 3. Proton derivation line shape observed at 4.2 °K in a single crystal of NH_4Br with $\vec{H}_0$ along [100] (curve a). Theoretical line shapes for $J=0$ (curve b) and $J=0.7$ (curve c) are calculated for the same orientation with $\langle\Delta H^2\rangle = 6\ G^2$. The modulation was 1 G. (The vertical scale is arbitrary.)

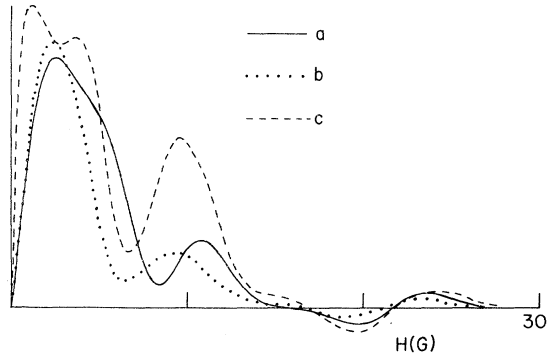

FIG. 4. Proton derivative line shapes observed (Ref. 12) for NH_4I powder after 3 h at 20 °K (curve b) and 10 h at 4.2 °K (curve c). Theoretical line shape for $\vec{H}_0$ along [100] is calculated for $J=3.3$ and $\langle \Delta H^2 \rangle = 3.5$ G^2 (curve a). The modulation is 0.5 G. (The vertical scale is arbitrary.)

intraionic dipolar energies (the perturbed Zeeman states) must be dropped from the calculation. This is the idea employed by Abragam and Kambe[10] for the broadening of pure quadrupole resonance lines. This additional truncation of the dipolar Hamiltonian results in a smaller broadening of the component lines in this "resolved" case over the Van Vleck case. Itoh *et al.*[2] have performed both calculations for NH_4Br with $\vec{H}_0$ in the [100] direction and found a broadening factor of about 7.5 G^2 for the Van Vleck case and about 3.3 G^2 for the resolved case of Abragam and Kambe. This latter broadening actually differs slightly for each component line but its average is about 3.3 G^2. Since the actual situation in NH_4Br is somewhere between these two extremes (components are partially resolved), they take a value somewhere between these two limits and find that 6 G^2 gives the best fit with experiment. This is the value we have employed in determining the theoretical line shapes in Fig. 3. Comparison of those with the observed line shape reveals that the $J=0$ situation is a very good description of the observed line shape except near the center of the resonance. This discrepancy near the center is clearly reduced in the $J=0.7$ case but only at the expense of the agreement elsewhere. In fact, it can be seen that any nonzero splitting in pushing one component out from, and another into, the origin will only serve to worsen the agreement in the wings. We must conclude from the excellent agreement just noted for $J=0$ over most of the line shape that the actual splitting in NH_4Br is still much less than the dipolar energy ($\Delta_3 \ll \Gamma_p$). Like Itoh *et al.*[2] we can offer no adequate explanation for the observed line shape near the center of the resonance but it would not seem to be a result of tunneling.

Below about 231 °K, NH_4I has the same tetragonal crystal structure as NH_4Br but with a slightly larger unit cell.[11] Lalowicz and Hennel[12] have measured the derivative of the proton absorption line shape for a polycrystalline sample of NH_4I at temperatures from 1.4 to 78 °K and find a slow variation with time as the sample is maintained at constant temperature. In Fig. 4 we reproduce the line shapes they obtained after 3 h at 20 °K (dotted line) and after 10 h at 4.2 °K (dashed line). These are compared with the theoretical line shape for a single crystal with $\vec{H}_0$ along [100] (i.e., the ionic x axis) and with $J=3.3$ (full line). As in the case of the bromide the actual broadening factor should be between the Van Vleck case and the resolved component case of Abragam and Kambe. These two limits in NH_4Br were 7.5 and 3.3 G^2 for $\vec{H}_0$ along [100]. Now the proton contribution (which is the only significant one) to the Van Vleck interionic second moment in NH_4I is easily calculated from the structure[11] to be about 4.5 G^2. This is the upper limit of the broadening. Now since this tetragonal structure of NH_4I is the same as that of NH_4Br, the lower limit of the broadening, corresponding to the resolved component case, must be about 2 G^2. Therefore we can say that in NH_4I the broadening factor should be between 2 and 4.5 G^2. In light of this, the chosen broadening factor of 3.5 G^2 in Fig. 4 is not unreasonable. For a smaller broadening the twin nature of the central peak would become more pronounced (cf. Fig. 2).

The comparison of a signal obtained with a polycrystalline sample to that calculated for a single-crystal orientation also requires some discussion. Let us specify the direction of $\vec{H}_0$ in the coordinate system of Fig. 1 by the spherical angular coordinates (θ, ϕ), i.e., θ is the angle $\vec{H}_0$ makes with the z axis and ϕ is the angle which the projection of $\vec{H}_0$ on the xy plane makes with the x axis. Where a given component line occurs in the spectrum is a function of these angles, $H=H(\theta, \phi)$ and can be calculated for any arbitrary (θ, ϕ) by the machinery previously developed. If we knew this function $H(\theta, \phi)$ we could calculate the powder spectrum by taking a polycrystalline average. The intensity, $g(H)\Delta H$, of the powder line between H and $H+\Delta H$ is proportional to the number of crystallites so oriented as to give a component line in this range,[3,4] i.e.,

$$g(H)\Delta H \alpha \int_R \sin\theta \, d\theta \, d\phi \ ,$$

where the region of integration R is such that $H < H(\theta, \phi) < H+\Delta H$.

This can be written as

$$g(H)\alpha \int_R \left(\frac{\partial H}{\partial \phi}\right)^{-1} \sin\theta \, d\theta \ .$$

The integrand of this expression becomes in-

finite and produces an infinity in the powder spectrum when $H(\theta, \phi)$ is at a maximum, since then $(\partial H/\partial\phi)=0$. Now $H(\theta, \phi)$ is at a maximum, or two lines are degenerate when $\vec{H}_0$ is along a twofold symmetry axis of the ion, e.g., consider $\vec{H}_0$ along the x axis so that $\theta=\frac{1}{2}\pi$, $\phi=0$. Letting $\phi \rightarrow \delta\phi$ must result in the same spectral positions as letting $\phi \rightarrow -\delta\phi$, since the latter situation can be obtained from the former by a twofold rotation of the whole system about the x axis, which cannot itself alter the spectrum. Therefore, the component lines at $H(\frac{1}{2}\pi, 0)$, if they are not degenerate, must be a maximum with respect to changes in ϕ. Note, however, that for this particular direction, the same argument also applies to small changes in θ and shows that $H(\frac{1}{2}\pi, 0)$ is also a maximum with respect to θ.

Even after broadening the powder spectrum by the interionic broadening factor, one still expects to find peaks at the maximum values of $H(\theta, \phi)$. Since these occur for $\vec{H}_0$ along symmetry directions such as [100] (the ionic x axis) in NH_4I, we expect the single-crystal spectrum for this orientation to be at least qualitatively similar to the powder spectrum. An example of this similarity in the case where the theoretical powder spectrum is calculable is provided in the theory of spin isomerism.[4] This argument has been necessitated, of course, because an analytical solution for $H(\theta, \phi)$ is not tractable in the general case.

In view of the foregoing remarks, the agreement between the experimental line shape (particularly at 20 °K) and the theoretical one for $J=3.3$ (Fig. 4) is gratifying. This determination of the splitting parameter J should be compared with an analogous determination for a tunneling methyl group in CH_3CD_2I.[13] However, the latter is equivalent to the one-dimensional case of the three-dimensional problem treated in this paper. NMR lineshape analyses of this kind appear to be the only method for measuring tunneling splittings as small as the dipolar linewidth (typically 10–100 kHz) in solids.

Now, with no dipolar interaction J^A, J^E are the spatial splittings of the A and E states relative to the F state [Eqs. (16)]. So, from Eq. (18), J is a measure of the splitting between A and E states compared to the dipolar energy Γ_p. Hence, since $J=3.3$ gives a good fit with experiment for NH_4I as demonstrated in Fig. 4, we can say that in this material $J^A - J^E \sim \Gamma_p \sim 10^{-6}$ °K in temperature units. Therefore, the Boltzmann factor can have no effect on the relative populations of the A and E states at the lowest temperatures under discussion (~4 °K). However, Lalowicz and Hennel[12] interpret the slow changes observed in their line shape to spin conversion from the A (and E) species to the F species, so increasing the amount of F component present. This is consistent with the increased intensity at 4.2 °K of the peak at $1.5\ \Gamma_p/\gamma_p\hbar$ (i.e., 9 G) in Fig. 4, since this is associated with the F species [Eq. (17c)]. However, for the effects of spin conversion to be apparent at this temperature, the splitting J^A between A and F states [Eqs. (16)] must be at least of the order 1 °K, i.e., J^A, $J^E \gg J^A - J^E$. If this interpretation is correct, then the wave-function overlap necessary to achieve such a splitting may not be negligibly small. In this case, the approximation adopted of neglecting matrix elements of $\mathcal{H}'_{pp}$ between states of different orientation may begin to break down. The qualitative effect of a larger overlap would be to average the terms B_{ij} over a finite region of (θ, ϕ) space so reducing the value of every matrix element in Tables IV and V. Diagonalization would then lead to component lines closer to the center of the resonance. This is in the direction necessary to improve agreement between theory and experiment in Fig. 4.

Of course, if the overlap is too large then torsional oscillator states are not appropriate as a description of the spatial wave functions. This is probably the reason that this theory does not give adequate agreement with the observed line shapes in materials such as $(NH_4)_2SnCl_6$ reported previously.[4] The extremely narrow line shapes of such materials exhibit no peak as far out as $1.5\ \Gamma_p/\gamma_p\hbar$ and it seems probable that their low activation energies lead to significant delocalization of the ionic orientation so that a theory based on torsional oscillator states would not apply. A more fruitful approach in this case would seem to be a description of the spatial wave function in terms of free rotor states. Work along these lines is currently in progress.

APPENDIX A: NORMALIZING FACTORS

Consider the state given in Eq. (3a):

$$\psi^A = N_A^{-1/2} \sum_R \psi(R) .$$

If ψ^A is to be normalized then

$$N_A = \sum_{R_1} \sum_{R_2} \langle \psi(R_1) | \psi(R_2) \rangle = \sum_{R_1} \sum_{R_2} \langle \psi(E) | \psi(R_1^{-1} R_2) \rangle$$

because matrix elements are invariant under rotations, being simple numbers. Making the substitution $R = R_1^{-1} R_2$ we have

$$N_A = 12 \sum_R \langle \psi(E) | \psi(R) \rangle . \tag{A1}$$

Now, if the crystal field is at least tetrahedral all twofold rotations (C_2) are equivalent and all threefold rotations (C_3) are equivalent so that

$$N_A = 12(1 + 3s_2 + 8s_3) ,$$

where

$$s_2 = \langle \psi(E) | \psi(C_2) \rangle , \quad s_3 = \langle \psi(E) | \psi(C_3) \rangle .$$

Similarly, for the other states of Eqs. (3), N_E and N_F can be found.

Suppose, however, that the crystal field is not tetrahedral, but tetragonal, with the tetragonal axis along z. Then all C_3 axes are still equivalent because they can all be transformed into one another by rotations around the tetragonal axis, and $C_2(x)$ is equivalent to $C_2(y)$ for the same reason. Then we can write

$$\begin{aligned} &\langle \psi(E) | \psi(C_2(x)) \rangle = \langle \psi(E) | \psi(C_2(y)) \rangle = s_2' , \\ &\langle \psi(E) | \psi(C_2(z)) \rangle = s_2 , \end{aligned} \tag{A2}$$

while s_3 are the same as before.

Hence we find from Eq. (A1)

$$N_A(\text{tetragonal}) = 12(1 + s_2 + 2s_2' + 8s_3)$$

and similarly,

$$N_E(\text{tetragonal}) = 12(1 + s_2 + 2s_2' - 4s_3) ,$$

$$N_{Fn} = \sum_{R_1} \sum_{R_2} \langle \psi(R_1) | \psi(R_2) \rangle D_{ni}(R_1^{-1}) D_{ni}(R_2^{-1})$$

$$= 4(1 - s_2) \qquad \text{for } n = 1, 2$$

$$= 4(1 + s_2 - 2s_2') \quad \text{for } n = 3 .$$

APPENDIX B: MATRIX ELEMENTS OF $\mathcal{H}_R$

$\mathcal{H}_R$ is diagonal in the representation chosen. Consider the diagonal element of Eq. (8a):

$$H^A = \langle \Psi^{Am} | \mathcal{H}_R | \Psi^{Am} \rangle = \langle \psi^A | \mathcal{H}_R | \psi^A \rangle$$

from Eq. (4a) since $\mathcal{H}_R$ is a function of spatial variables only. Substituting from Eq. (3a),

$$H^A = N_A^{-1} \sum_{R_1} \sum_{R_2} \langle \psi(R_1) | \mathcal{H}_R | \psi(R_2) \rangle$$

$$= N_A^{-1} \sum_{R_1} \sum_{R_2} \langle \psi(E) | \mathcal{H}_R | \psi(R_1^{-1} R_2) \rangle$$

because both the matrix element and $\mathcal{H}_R$ are invariant under the operations R_1, R_2. Substituting $R = R_1^{-1} R_2$ we have

$$H^A = 12 N_A^{-1} \sum_R \langle \psi(E) | \mathcal{H}_R | \psi(R) \rangle .$$

Now, if the crystal field is at least tetrahedral we can write

$$\Delta_2 = \langle \psi(E) | \mathcal{H}_R | \psi(C_2) \rangle , \quad \Delta_3 = \langle \psi(E) | \mathcal{H}_R | \psi(C_3) \rangle ,$$

$$H_t = \langle \psi(E) | \mathcal{H}_R | \psi(E) \rangle$$

(cf. Appendix A), whence

$$H^A = (H_t + 3\Delta_2 + 8\Delta_3)/(1 + 3s_2 + 8s_3)$$

and similarly for the other elements H^E and H^F.

However, if the crystal field is not tetrahedral but tetragonal we must write, in analogy to (A2),

$$\langle \psi(E) | \mathcal{H}_R | \psi(C_2(x)) \rangle = \langle \psi(E) | \mathcal{H}_R | \psi(C_2(y)) \rangle = \Delta_2' ,$$

$$\langle \psi(E) | \mathcal{H}_R | \psi(C_3) \rangle = \Delta_3 .$$

Then we find

$$H^A(\text{tetragonal}) = (H_t + \Delta_2 + 2\Delta_2' + 8\Delta_3)/(1 + s_2 + 2s_2' + 8s_3)$$

and similarly,

$$H^E(\text{tetragonal}) = (H_t + \Delta_2 + 2\Delta_2' - 4\Delta_3)/(1 + s_2 + 2s_2' - 4s_3) ,$$

$$H_n^F = \langle \Psi_n^{Fm} | \mathcal{H}_R | \Psi_n^{Fm} \rangle$$

$$= (H_t - \Delta_2)/(1 - s_2), \qquad n = 1, 2$$

$$= (H_t + \Delta_2 - 2\Delta_2')/(1 + s_2 - 2s_2') , \quad n = 3 .$$

Now if we reduce the matrix for $\mathcal{H}_R$ by H_1^F [1], where [1] is the unit matrix [cf. Eqs. (16)] the new diagonal elements become, for the limit of small overlap,

$$\begin{aligned} J^A &= H^A - H_1^F = 2(\Delta_2 + \Delta_2' + 4\Delta_3) , \\ J^E &= H^E - H_1^F = 2(\Delta_2 + \Delta_2' - 2\Delta_3) , \\ J_{1,2}^F &= H_{1,2}^F - H_1^F = 0 , \\ J_3^F &= H_3^F - H_1^F = 2(\Delta_2 - \Delta_2') . \end{aligned} \tag{B1}$$

Note that if the crystal field is only slightly distorted along z, J_3^F is very small.

---

*Work supported by the Defense Research Board of Canada and the National Research Council of Canada.

[1] R. Bersohn and H. S. Gutowsky, J. Chem. Phys. 22, 651 (1954).

[2] J. Itoh, R. Kusaka, and Y. Saito, J. Phys. Soc. Japan 17, 463 (1962).

[3] K. Tomita, Phys. Rev. 89, 429 (1953).

[4] A. Watton, A. R. Sharp, H. E. Petch, and M. M. Pintar, Phys. Rev. B 5, 4281 (1972); A. Watton, thesis (McMaster University, 1971) (unpublished).

[5] F. Apaydin and S. Clough, J. Phys. C 1, 932 (1968).

[6] Many of the group-theoretical techniques employed in this work can be found in, for example, M. Hamermesh, *Group Theory* (Addison-Wesley, Reading, Mass., 1962).

[7] T. Nagamiya, Progr. Theoret. Phys. (Kyoto) 6, 702 (1951).

[8] A. Bonilla, C. W. Garland, and N. E. Schumaker, Acta Cryst. A26, 156 (1970).

[9] H. A. Levy and S. W. Peterson, J. Am. Chem. Soc. 75, 1536 (1953).

[10] A. Abragam and K. Kambe, Phys. Rev. 91, 894 (1953).

[11] V. Hovi, K. Paarvola, and E. Nurmi, Ann. Acad. Sci. Fennicae, Ser. A VI, 328 (1969).

[12] Z. T. Lalowicz and J. W. Hennel, Acta Phys. Polon. A40, 547 (1971).

[13] C. Mottley, T. B. Cobb, and C. S. Johnson, Jr., J. Chem. Phys. 55, 5823 (1971).